Acta Crystallographica Section D
Biological Crystallography
ISSN 0907-4449

Crystallization of the bovine ADP/ATP carrier is critically dependent upon the detergent-to-protein ratio

Cécile Dahout-Gonzalez,[a] Gérard Brandolin[a]* and Eva Pebay-Peyroula[b]*

[a]Laboratoire de Biochimie et Biophysique des Systèmes Intégrés, UMR 5092 CEA–CNRS–Université Joseph Fourier, Département de Réponse et Dynamique Cellulaires, CEA-Grenoble, 17 Avenue des Martyrs, F-38054 Grenoble CEDEX 9, France, and [b]Institut de Biologie Structurale, UMR 5075 CEA–CNRS–Université Joseph Fourier, 41 Rue Jules Horowitz, F-38027 Grenoble CEDEX 1, France

Correspondence e-mail: gbrandolin@cea.fr, pebay@ibs.fr

Received 25 July 2003
Accepted 18 September 2003

The ADP/ATP carrier is an integral membrane protein located in the mitochondrial inner membrane. It mediates the exchange of cytosolic ADP for ATP generated in the mitochondrial matrix. Here, the purification and crystallization of the bovine ADP/ATP carrier in complex with the inhibitor carboxyatractyloside in the presence of LAPAO, an aminoxide detergent, is reported. High-quality crystals were only obtained when excess detergent was removed to reach a controlled detergent-to-protein ratio.

1. Introduction

In eukaryotic cells, ATP generated by the oxidative phosphorylation process in the mitochondrial matrix is exported towards the cytoplasm in exchange for an ADP molecule by the adenine nucleotide carrier. Therefore, the mitochondrial ADP/ATP carrier plays a crucial role in the energetic metabolism of the entire cell. Dysfunction of the carrier results in severe disorders such as myopathies (Graham *et al.*, 1997) or ophtalmoplegias (Kaukonen *et al.*, 2000). Recently, it was also proposed to be involved in the mitochondrial permeability transition (for a review, see Belzacq *et al.*, 2002). The ADP/ATP carrier belongs to the mitochondrial carrier family (for a review, see Walker & Runswick, 1993). Like all the members of this family, it is a nuclear-encoded protein of about 300 amino-acid residues characterized by a threefold repeat motif of 100 residues. The ADP/ATP carrier is one of the best characterized members of this family for two main reasons. Firstly, it is abundant, amounting to 10% of the inner membrane protein in heart mitochondria. Secondly, it can be specifically inhibited by two powerful natural inhibitors, carboxyatractyloside (CATR) and bongkrekic acid (BA), that bind with high affinity to the carrier. Chemical, immunochemical, enzymatic and fluorimetric approaches led to the conclusion that CATR– and BA–carrier complexes adopt stable conformations that correspond to two conformations of the carrier adopted during adenine nucleotide transport (for a review, see Fiore *et al.*, 1998).

Membrane-protein crystallization is still a bottleneck in the elucidation of high-resolution structures, as can be seen from the small number of known structures (for a review, see White, 2003). The classical approach consists of solubilizing proteins in detergent micelles and then adding a precipitant in a similar way to the approach for soluble proteins. The preparation of pure and functional membrane proteins in detergent is still challenging and the role of lipids is probably crucial during this step (for a review, see Pebay-Peyroula & Rosenbusch, 2001). Use of lipidic cubic phases was shown to be an interesting alternative approach, as the lipidic environment of the protein is maintained during crystallization (Landau & Rosenbusch, 1996). Furthermore, concentration of the protein solution to 10 mg ml^{-1}, a typical value for crystallization, leads to the concomitant concentration of the detergent. This is commonly observed for membrane proteins as detergent micelle sizes do not significantly differ from mixed micelle sizes. A large amount of detergent in the final solution may destabilize the protein and prevent crystallization occurring. Detergent removal has been addressed in the two-dimensional crystallization of membrane proteins. In this case, total detergent removal in the presence of lipids drives the crystallization process and can be performed by the use of polystyrene beads (Rigaud *et al.*, 1997; Lacapère *et al.*, 1998).

In this paper, we present an approach that allowed the removal of excess detergent and control of the detergent-to-protein ratio in three-dimensional crystallization. We describe the purification and crystallization of the ADP/ATP carrier complexed with CATR. The approach described here allowed solution of the structure at 2.2 Å resolution (Pebay-Peyroula *et al.*, 2003). We show that the amount of detergent present in the protein preparation is a critical parameter for obtaining crystals suitable for X-ray diffraction analysis. Two crystal forms were obtained, one of which presented a defect that we were able to analyze retrospectively.

2. Purification

Bovine mitochondria were isolated from heart muscle by differential centrifugations (Smith,

1967), suspended in 0.27 *M* sucrose, 2 m*M* Tris pH 7.4 and stored in liquid nitrogen. 50 mg of mitochondrial proteins were suspended at 10 mg ml^{-1} in a medium consisting of 500 m*M* NaCl, 10 m*M* Tris pH 7.4, 1 m*M* EDTA. Mitochondria were incubated in the presence of 20 µ*M* CATR for 10 min at 273 K and then lysed by the addition of 2%(*w*/*v*) 3-laurylamido-*N*,*N*′-dimethylpropylaminoxyde (LAPAO), a detergent synthesized as described in Brandolin *et al.* (1980). The critical micellar concentration of LAPAO was determined to be 1.3 m*M* by fluorimetry (De Vendittis *et al.*, 1981). Purification of the CATR–carrier complex was carried out by hydroxylapatite (HTP) chromatography according to Krämer *et al.* (1977). In bovine heart mitochondria, the protein is exclusively present as isoform T1 (unpublished results). HTP (BioRad) was equilibrated in a medium made up of 100 m*M* NaCl, 10 m*M* Tris pH 7.4, 1 m*M* EDTA, 0.05%(*w*/*v*) LAPAO. The flowthrough fraction was collected and submitted to gel-filtration chromatography using Ultrogel AcA202 resin (BioSepra) equilibrated in 10 m*M* Tris pH 7.4, 1 m*M* EDTA, 0.05% LAPAO supplemented with either 5 or 100 m*M* NaCl. The protein was concentrated on a Centricon YM30 device (Amicon) to about 10 mg ml^{-1}.

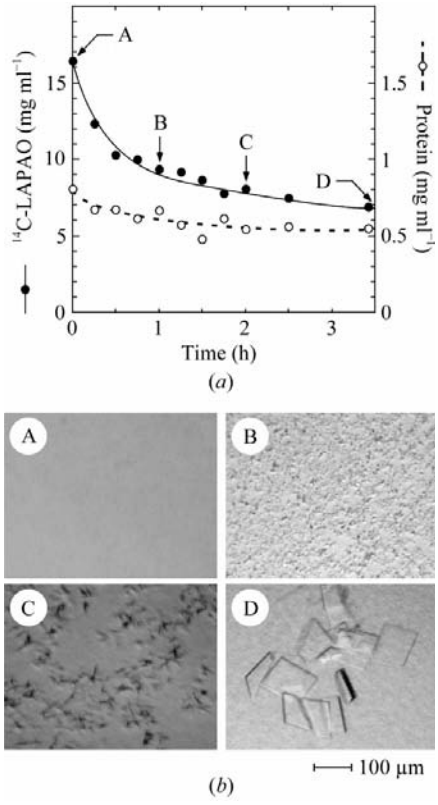

Figure 1
Effect of the LAPAO-to-protein ratio on ADP/ATP carrier crystallization. (*a*) Time course of ^{14}C-LAPAO removal. Purified bovine carrier (0.8 mg ml^{-1}) was incubated in the presence of 100 mg of SM2 Bio-Beads per milligram of protein at 277 K. The radioactivity associated with aliquots of the supernatant was quantified by liquid-scintillation counting (full line) and the amount of protein was quantified using the bicinchoninic reagent kit (dotted line). (*b*) Crystallization experiments in the presence of 2-methyl-2,4-pentanediol. Protein was sampled during the Bio-Beads treatment at steps A, B, C, D shown in (*a*) with detergent-to-protein ratios of 20, 16, 13 and 10 g detergent per gram of protein, respectively.

Table 1
Crystallization conditions and crystallographic data for the two crystal forms of the bovine ADP/ATP carrier.

The table illustrates the three types of unit cell determined during data processing. Two crystal forms were obtained, $C222_1$ and $P2_12_12_1$. In the primitive crystal form, 90% of crystals present a defect that doubles the *c* parameter, as shown in the third row.

NaCl concentration in the protein solution (m*M*)	Crystallization conditions	Space group	Unit-cell parameters (Å)	Resolution (Å)
5	30% Jeffamine M600, 20 m*M* $NiSO_4$, 100 m*M* HEPES pH 7.0	$C222_1$	*a* = 79.874, *b* = 109.163, *c* = 89.315	25–2.8
100	30% Jeffamine M600, 5 m*M* Na citrate, 100 m*M* Tris pH 8.5	$P2_12_12$	*a* = 85.437 *b* = 83.463 *c* = 49.922	25–2.2
100	30% Jeffamine M600, 5 m*M* Na citrate, 100 m*M* Tris pH 8.5	$P2_12_12$	*a* = 86.200 *b* = 85.740 *c* = 101.690	25–2.7

3. Crystallization

Initial crystallization trials were carried out in hanging drops by the vapour-diffusion method using commercial screens (Hampton Research). Small needles were obtained in the presence of alcohols (*t*-butanol, ethanol or 2-methyl-2,4-pentanediol), but crystal growth was hindered by the excess of detergent. In order to decrease the detergent-to-protein ratio, the protein solution prior to concentration was incubated in the presence of moist activated SM2 Bio-Beads (Bio-Rad; 100 mg per milligram of protein; Holloway, 1973). The time course of ^{14}C-LAPAO removal was followed by radioactivity measurements and the protein concentration was assessed by the bicinchoninic acid reagent kit (Sigma) using bovine serum albumin as a standard. As shown in Fig. 1(*a*), the detergent concentration decreased rapidly during the first half hour of incubation and slowly afterwards, whereas the protein concentration remained quite constant. As a result, the detergent-to-protein ratio decreased from 20 to 10 g per gram of protein. The crystallization process was followed as a function of the detergent-to-protein ratio (Fig. 1*b*). Protein crystals appeared when the ratio was decreased to about 13 g of LAPAO per gram of protein. A further decrease led to larger crystals, but 10 g per gram of protein was the lowest limit that could be reached while avoiding irreversible precipitation of the protein during the subsequent concentration step. This value was unexpected, as membrane proteins have been reported to retain 1–2 g of detergent per gram of protein (Möller & le Maire, 1993).

In order to grow crystals of high diffraction quality, new crystallization conditions were screened with a protein solution corresponding to D in Fig. 1(*a*). Single crystals (about 100 × 20 × 5 µm) appeared within 1–2 d at 293 K by mixing 1 µl protein solution with 1 µl reservoir solution. Two crystallization conditions were identified, depending on the initial NaCl concentration of the protein solution. In both cases, the reservoir contained 28–32% Jeffamine M600 (Hampton Research) as a precipitant and 20 m*M* $NiSO_4$, 100 m*M* HEPES pH 7.0 or 5 m*M* sodium citrate, 100 m*M* Tris pH 8.5 for protein solutions containing 5 or 100 m*M* NaCl, respectively (Table 1).

4. Crystal characterization

Crystals were flash-frozen in liquid nitrogen. Diffraction data were collected on beamlines BM30A, ID29, ID14-1 and ID14-2 at the European Synchrotron Radiation Facility, Grenoble. The data were processed using *DENZO*, *SCALEPACK* (Otwinowski & Minor, 1997) and programs from the *CCP*4 suite (Collaborative Computational Project, Number 4, 1994). More than 90% of the $P2_12_12$ crystals had a *c* parameter of 100 Å instead of 50 Å, with *a* and *b* remaining unchanged (Table 1). The corresponding Patterson functions displayed a very strong peak (over 40 r.m.s.d.) in the $z = 1/2$ section located at $x = 0$ and $y = 0.028$ (equivalent to 2.4 Å). We analyzed the mean intensities along each reciprocal axis and compared the intensities for odd and even values of the Miller indices. Fig. 2 represents the ratio of $\langle I(n_{\rm even})\rangle/\langle I(n_{\rm odd})\rangle$ as a function of resolution, *n* being *h*, *k* or *l*, respectively.

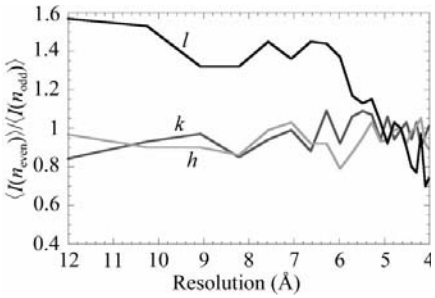

Figure 2
Intensity ratios of even over odd Miller indices as a function of resolution. The curves represent $\langle I(n_{even})\rangle/\langle I(n_{odd})\rangle$, where n is h, k or l for the light grey, grey and black curves, respectively. The mean intensities were calculated using the program *TRUNCATE* (Collaborative Computational Project, Number 4, 1994).

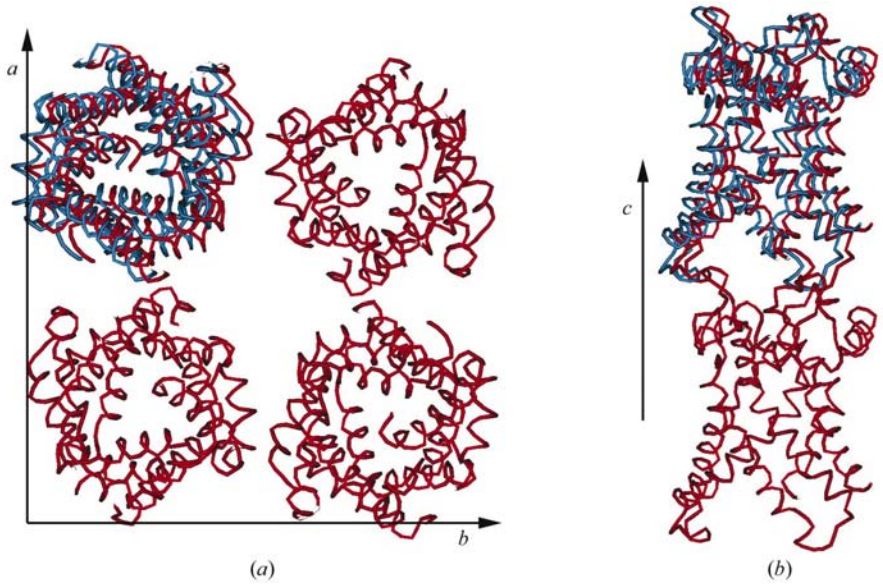

Figure 3
Packing in the primitive crystal form: (*a*) in the *ab* plane, (*b*) along the *c* axis. The unit cell shown has parameters $a = 85.437$, $b = 83.463$, $c = 49.922$ Å and corresponds to the red molecules. In the crystals where the *c* parameter is doubled, one layer along the *c* axis is displaced by 2.2 Å along *b* as shown by blue molecules. For the sake of clarity, only one blue molecule is shown in both panels.

These ratios are expected to be equal to one as seen for h and k; deviations denote either crystal defects or incorrect unit-cell parameters. In our case, additional spots were observed along c^*, double the c parameter, and therefore correspond to odd-numbered l indices. $\langle I(l_{odd})\rangle$ is expected to be weaker than $\langle I(l_{even})\rangle$. The ratios $\langle I(l_{even})\rangle/\langle I(l_{odd})\rangle$ observed among our crystals vary from infinity (perfect crystals with a 50 Å c parameter but treated with a 100 Å unit cell along c) to about 1.5. The values shown in Fig. 2 correspond to a typical crystal used in further analysis. Using the final model, molecular replacement (Navaza, 2001) on the primitive crystal form having the doubled c parameter showed that the crystal is built of layers stacked along the c axis, with one layer being slightly displaced along the b axis compared with crystals having the small c parameter. The displacement is shown in Fig. 3 and represents 2.2 Å, in agreement with the peak in the Patterson map. Together, these data suggest that the primitive crystal form favours defects by which, randomly within the crystal, one layer along the c axis is displaced by 2.2 Å along the b axis. As a result, the unit cell along c appears to be doubled and the Patterson function shows a strong peak that results from two molecules located at x, y, z and x, $y + 0.028$, $z + 1/2$. Because the defect is random, the ratio $\langle I(l_{even})\rangle/\langle I(l_{odd})\rangle$ is larger than 1 and varies from one crystal to another. Although a retrospective analysis of such crystals is interesting, the defects prevent the use of these crystals in solution of the protein structure. Therefore, the structure was solved by multiple isomorphous replacement from the centred crystal form using mercury derivatives. An initial molecular model was built from MIR phases and transposed to the primitive crystal for further refinement. The structure has been deposited with the PDB with accession code 1okc (Pebay-Peyroula *et al.*, 2003).

We thank the staff at the European Synchrotron Radiation Facilities and the French beamline BM30A (ESRF, Grenoble) for synchrotron support. We thank members of both laboratories for fruitful discussions.

References

Belzacq, A. S., Vieira, H. L., Kroemer, G. & Brenner, C. (2002). *Biochimie*, **84**, 167–176.
Brandolin, G., Doussière, J., Gulik, A., Gulik-Krzywicki, T., Lauquin, G. J. & Vignais, P. V. (1980). *Biochim. Biophys. Acta*, **592**, 592–614.
Collaborative Computational Project, Number 4 (1994). *Acta Cryst.* D**50**, 760–763.
De Vendittis, E., Palumbo, G., Parlato, G. & Bocchini, V. (1981). *Anal. Biochem.* **215**, 278–286.
Fiore, C., Trézéguet, V., Le Saux, A., Roux, P., Schwimmer, C., Dianoux, A. C., Noël, F., Lauquin, G. J., Brandolin, G. & Vignais, P. V. (1998). *Biochimie*, **80**, 137–150.
Graham, B. H., Waymire, K. G., Cottrell, B., Trounce, I. A., MacGregor, G. R. & Wallace, D. C. (1997). *Nature Genet.* **16**, 226–234.
Holloway, P. W. (1973). *Anal. Biochem.* **53**, 304–308.
Kaukonen, J., Juselius, J. K., Tiranti, V., Kyttala, A., Zeviani, M., Comi, G. P., Keranen, S., Peltonen, L. & Suomalainen, A. (2000). *Science*, **289**, 782–785.
Krämer, R., Aquila, H. & Klingenberg, M. (1977). *Biochemistry*, **16**, 4949–4953.
Lacapère, J.-J., Stokes, D. L., Olofsson, A. & Rigaud, J. L. (1998). *Biophys. J.* **75**, 1319–1329.
Landau, E. M. & Rosenbusch, J. P. (1996). *Proc. Natl Acad. Sci. USA*, **93**, 14532–14535.
Möller, J. V. & le Maire, M. (1993). *J. Biol. Chem.* **268**, 18659–18672.
Navaza, J. (2001). *Acta Cryst.* D**57**, 1367–1372.
Otwinowski, Z. & Minor, W. (1997). *Methods Enzymol.* **276**, 307–326.
Pebay-Peyroula, E. & Rosenbusch, J. P. (2001). *Curr. Opin. Struct. Biol.* **11**, 427–432.
Pebay-Peyroula, E., Dahout-Gonzalez, C., Kahn, R., Trézéguet, V., Lauquin, G. J.-M. and Brandolin G. (2003). In the press.
Rigaud, J.-L., Mosser, G., Lacapere, J.-J., Olofsson, A., Levy, D. & Ranck, J. L. (1997). *J. Struct. Biol.* **118**, 226–235.
Smith, A. L. (1967). *Methods Enzymol.* **10**, 81–86.
Walker, J. E. & Runswick, M. J. (1993). *J. Bioenerg. Biomembr.* **25**, 435–446.
White, S. H. (2003). *Membrane Proteins of Known Structure.* http://blanco.biomol.uci.edu/Membrane_Proteins_xtal.html.